Supplementary Information for

Surface Functionalized Manganese Ferrite Nanocrystals for Enhanced Uranium Sorption and Separation in Water

Seung Soo Lee,[a] Wenlu Li,[a] Changwoo Kim,[a] Minjung Cho,[b] Brandon J. Lafferty,[c] and John D. Fortner[a,*]

[a]Department of Energy, Environmental, and Chemical Engineering, Washington University, St. Louis, MO63130
[b]Department of Translational Imaging and Department of Nanomedicine, Houston Methodist Research Institute, Houston, TX77030
[c]U.S. Army Corps of Engineers, Engineer Research and Development Center, Vicksburg, MS39180
[*]corresponding: jfortner@wustl.edu

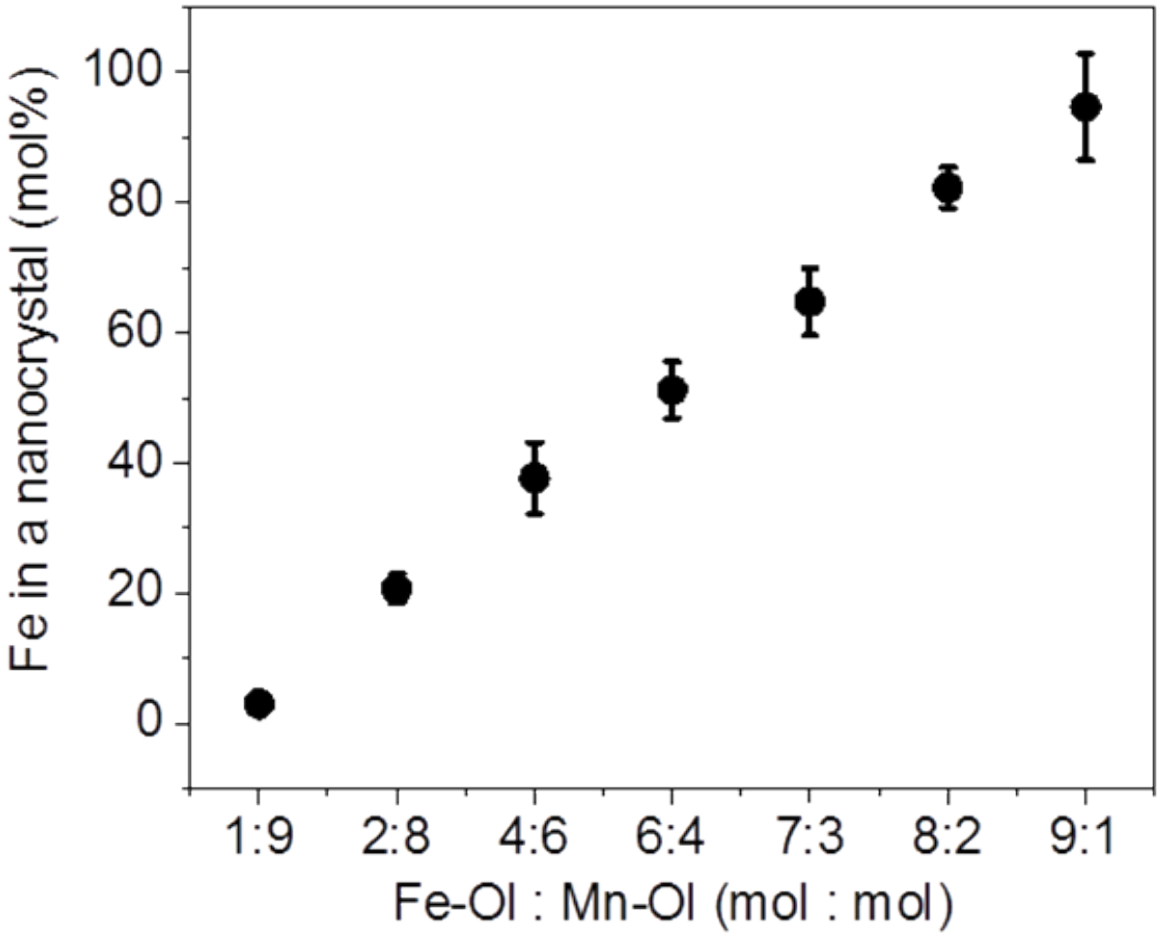

Fig S1. Composition control of manganese iron oxide nanocrystals. The molar percentage iron in the nanocrystal increases with elevated ratio of iron precursor (iron oleate, Fe-Ol) to manganese precursor (manganese oleate, Mn-Ol).

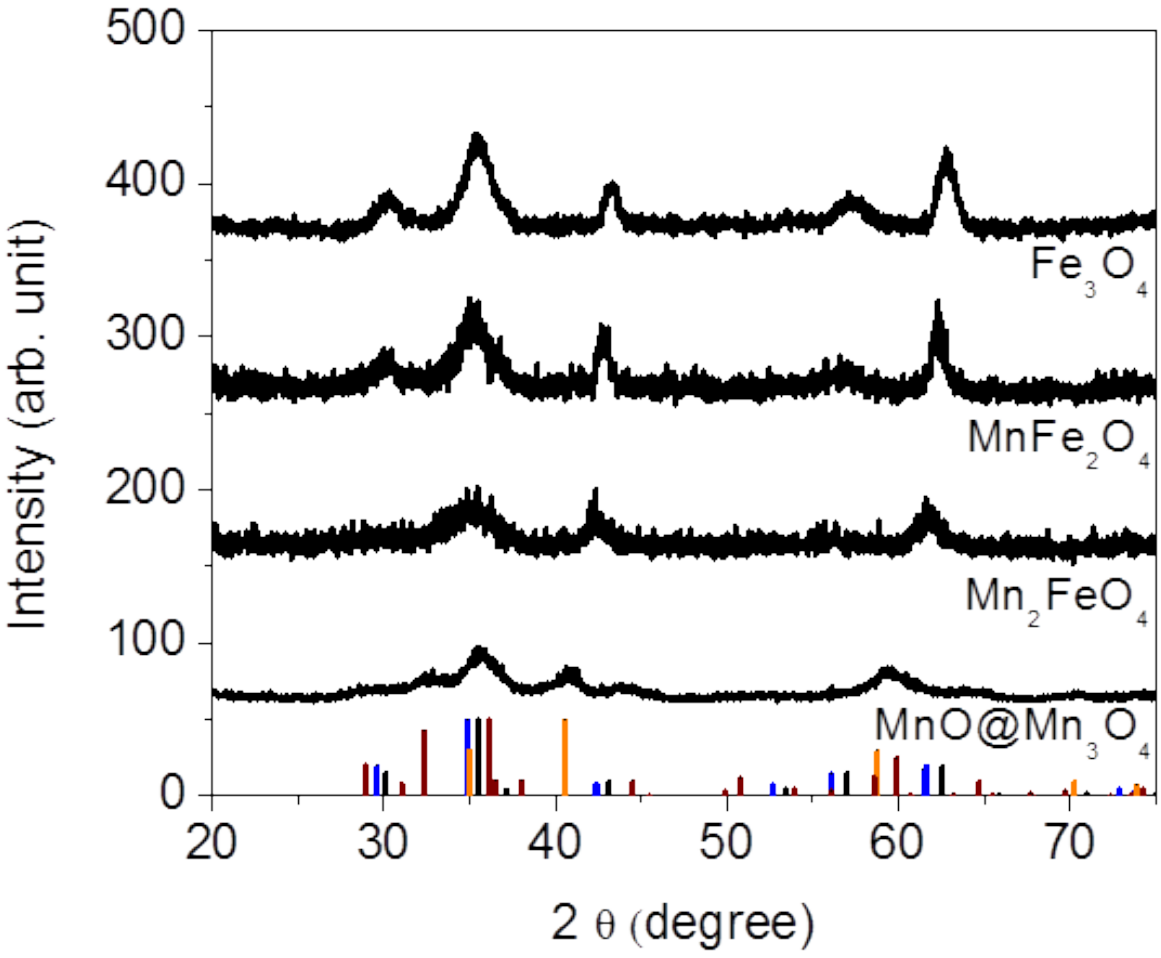

Fig S2. X-ray diffraction patterns of composition controlled manganese iron oxide nanocrystal samples. Peaks of manganese iron oxide samples ($MnFe_2O_4$ and Mn_2FeO_4) are shifted towards manganese oxide as the composition ratio of manganese to iron in the nanocrystal structure is increased. $MnFe_2O_4$; JCPDS # 38-0430 (blue)) manganese oxide phase ($MnO@Mn_3O_4$; JCPDS # 07-0230 (yellow) for MnO and JCPDS # 24-0734 (wine) for Mn_3O_4) from iron oxide phase (Fe_3O_4; JCPDS # 19-0629 (black).

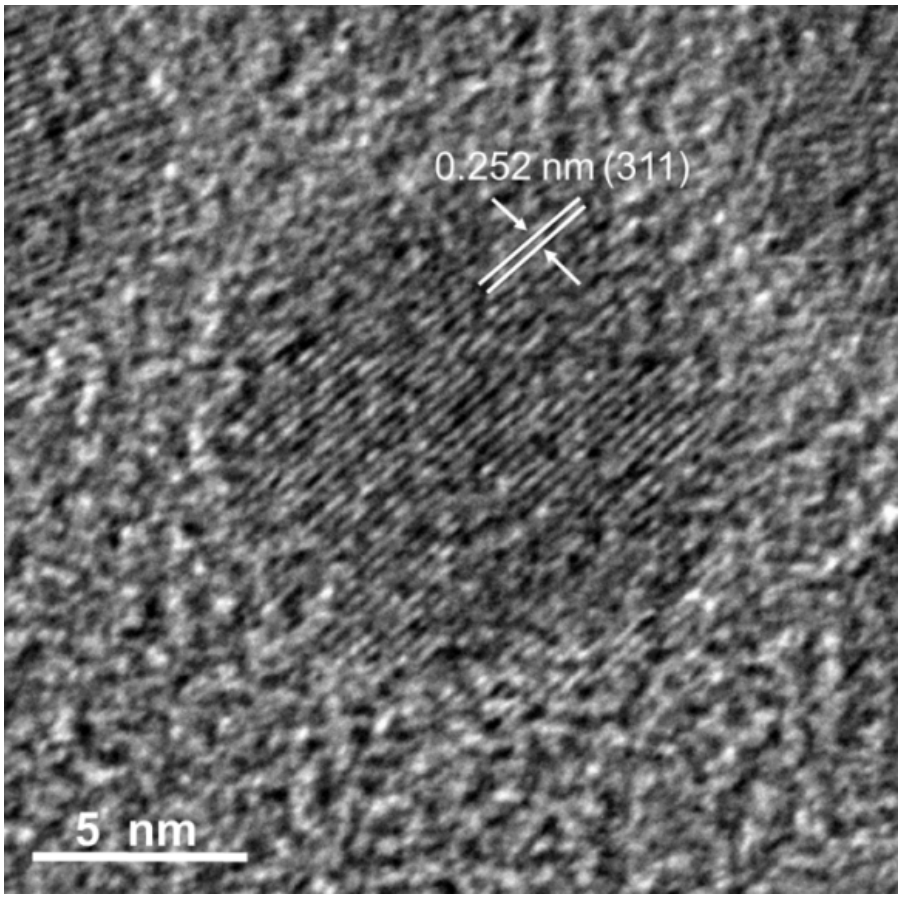

Fig S3. HR-TEM image of $MnFe_2O_4$ nanocrystals. The distance between crystal lattice fringes of 0.252 nm were indexed to (311) planes of $MnFe_2O_4$.

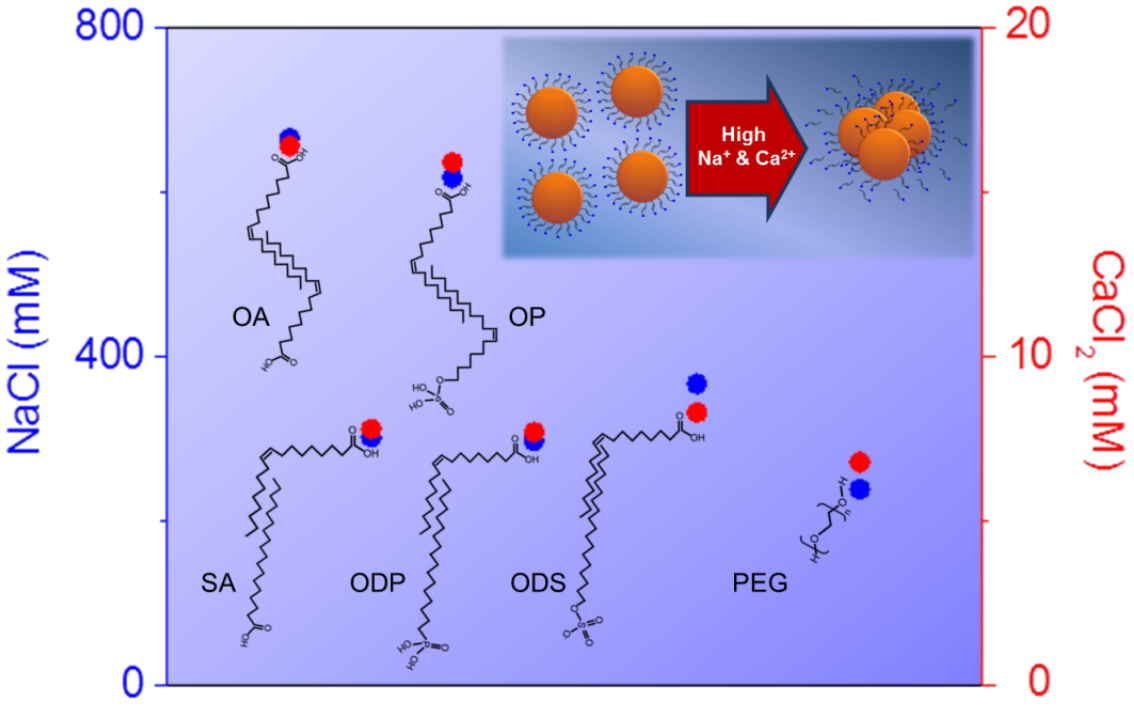

Fig S4. Attachment efficiency (α) as a function of mono-/di- valent salt concentrations (NaCl (blue) and $CaCl_2$ (red)) for both bilayered- and pegylated- $MnFe_2O_4$ nanocrystals. The attachment efficiency (α) for each nanocrystal sample was calculated by measuring the aggregation rates of the particles as a function of time and salt concentrations. The nanocrystal concentration employed was 2.5×10^{12}nanocrystals/L. The inset image shows nanocrystal aggregation at high ionic strength condition.

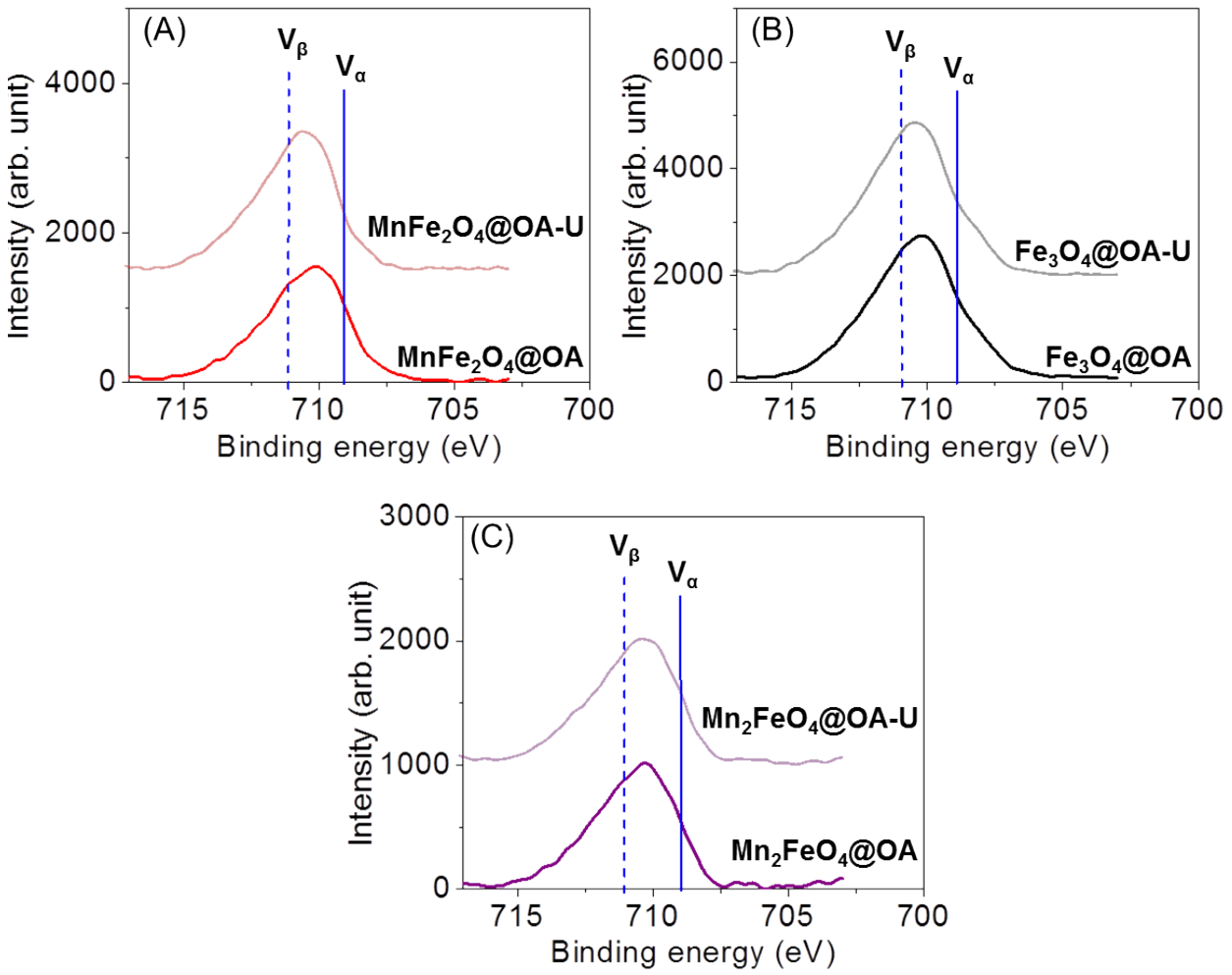

Fig S5. Redox reaction of iron (Fe) on the surface of the nanocrystals before and after uranium sorption measurement. Iron 2P XPS data was used to evaluate the ratio of Fe(II)/Fe(III) calculated by $(V_\alpha)/(V_\beta)$ from the sample ($MnFe_2O_4$@OA, (A); Fe_3O_4@OA, (B); Mn_2FeO_4@OA, (C)) before and after the uranium sorption measurement (Table S6)

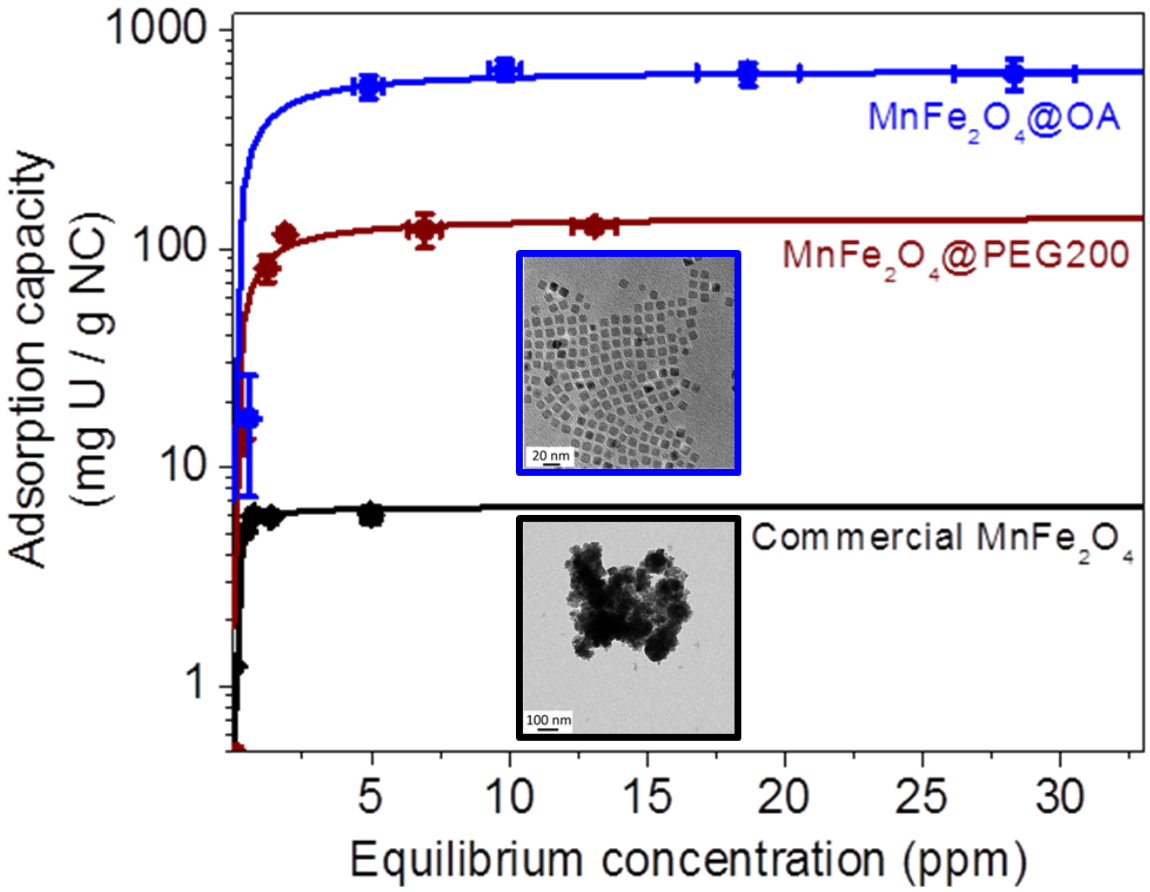

Fig S6. Uranium sorption isotherm on both engineered and commercial $MnFe_2O_4$ nanocrystals. Uranium sorption measurements were performed on engineered nanocrystalline $MnFe_2O_4$ (oleic acid bilayered (blue) and pegylated (single layered, dark red); typical nanocrystal concentration was 2.3×10^{15} nanocrystals in each sample) and commercial $MnFe_2O_4$ nanocrystals (average size of the nanocrystals were 50 nm) at uranium (U(VI)) concentration from 0.1 to 40 mg/L at pH 7.0. All calculated uranium sorption capacity values were fitted by Langmuir isotherm equation (solid lines).

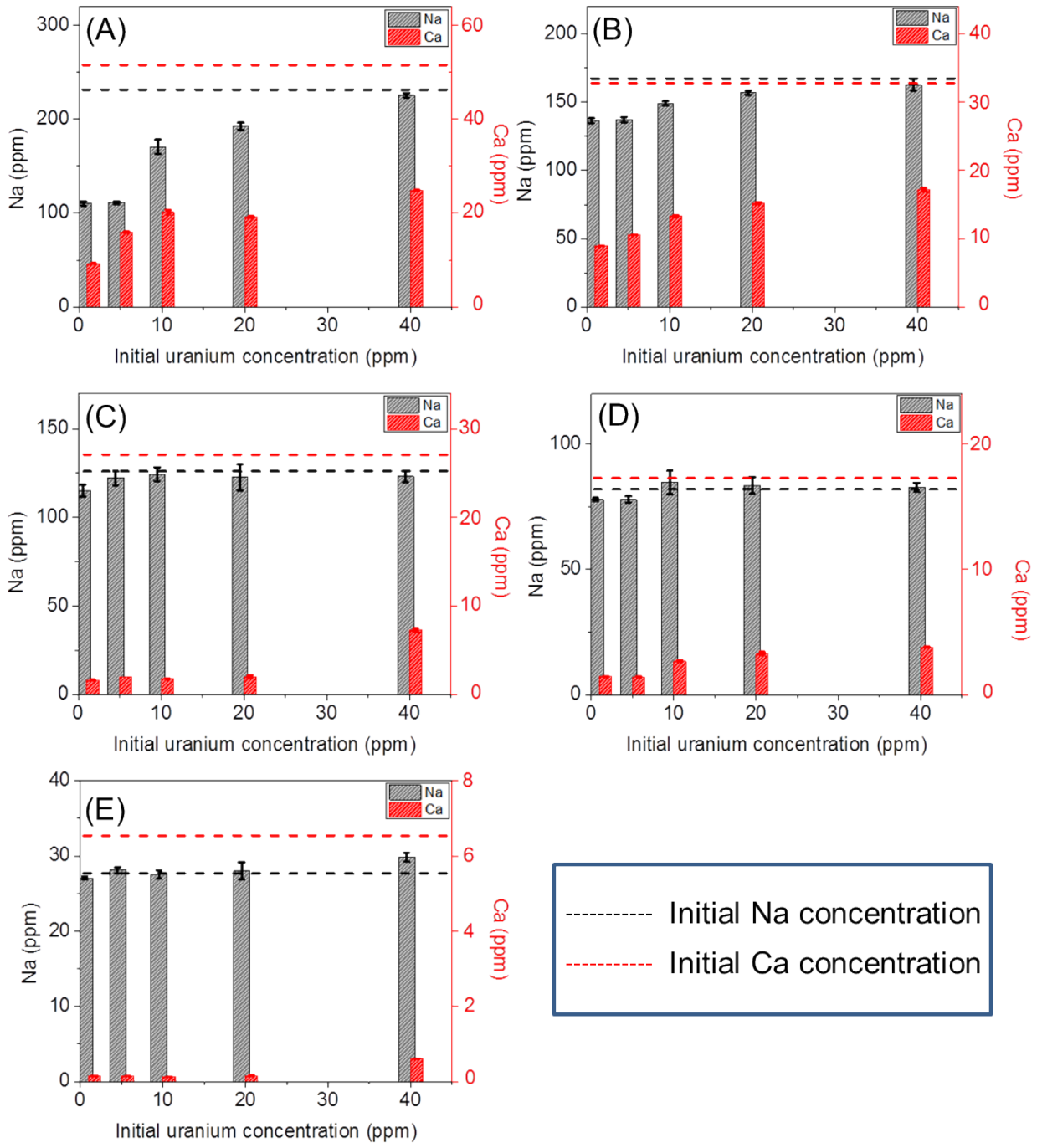

Fig S7. Multi-sorbate experiments including sodium and calcium as well as uranium. The remaining sodium (gray) and calcium (red) concentrations in the supernatant samples after uranium sorption on $MnFe_2O_4$@OP samples (8.436 mg/L of the nanocrystals) at elevated sodium and calcium concentrations were measured at pH 7 by ICP-OES. The ratio of the initial sodium (dot black lines) and calcium (dot red lines) concentration was 235.4/51.3 (A), 167/32.7 (B), 127.7/27.2 (C), 80.6/17.4 (D), and 23.8/6.5 ppm (E), respectively.

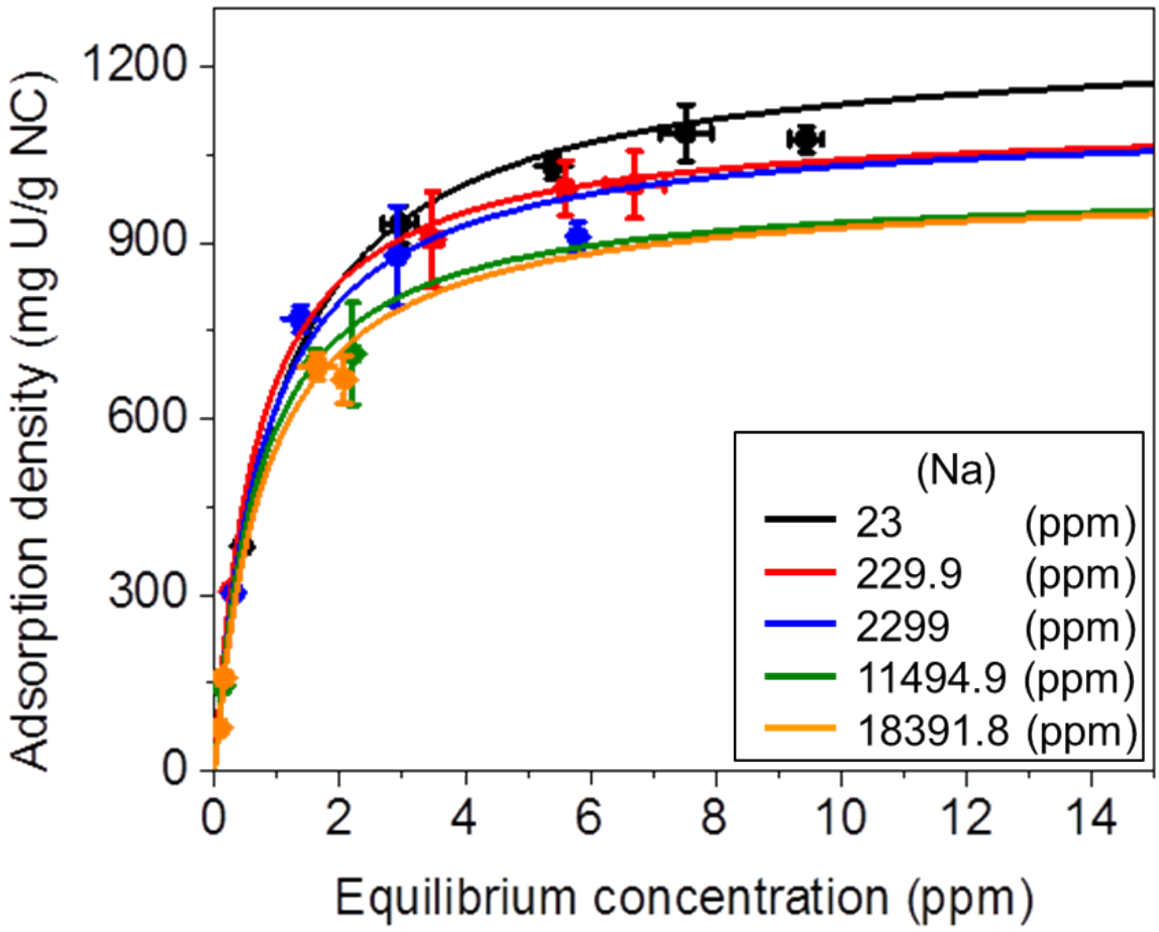

Fig S8. Uranium sorption isotherm on $MnFe_2O_4$@OP nanocrystals at elevated sodium concentrations. Typical nanocrystal concentration was 2.3×10^{15} nanocrystals/L in each sample at uranium (U(VI)) concentration from 0.1 to 40 mg/L at pH 7.0. All calculated uranium sorption capacity values were fitted by Langmuir isotherm equation.

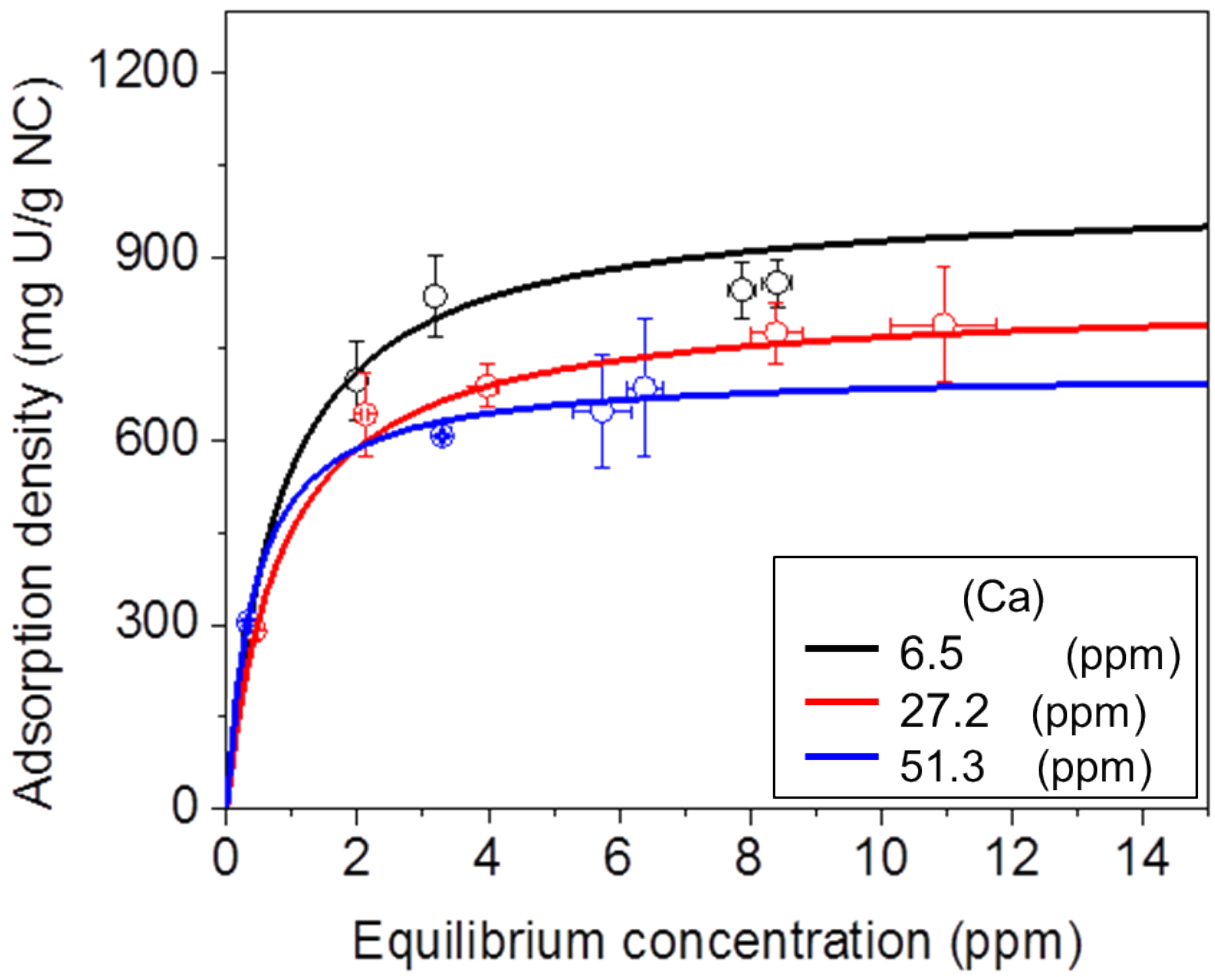

Fig S9. Uranium sorption isotherm on $MnFe_2O_4$@OP nanocrystals at elevated calcium concentrations. Typical nanocrystal concentration was 2.3×10^{15} nanocrystals/L in each sample at uranium (U(VI)) concentration from 0.1 to 40 mg/L at pH 7.0. All calculated uranium sorption capacity values were fitted by Langmuir isotherm equation.

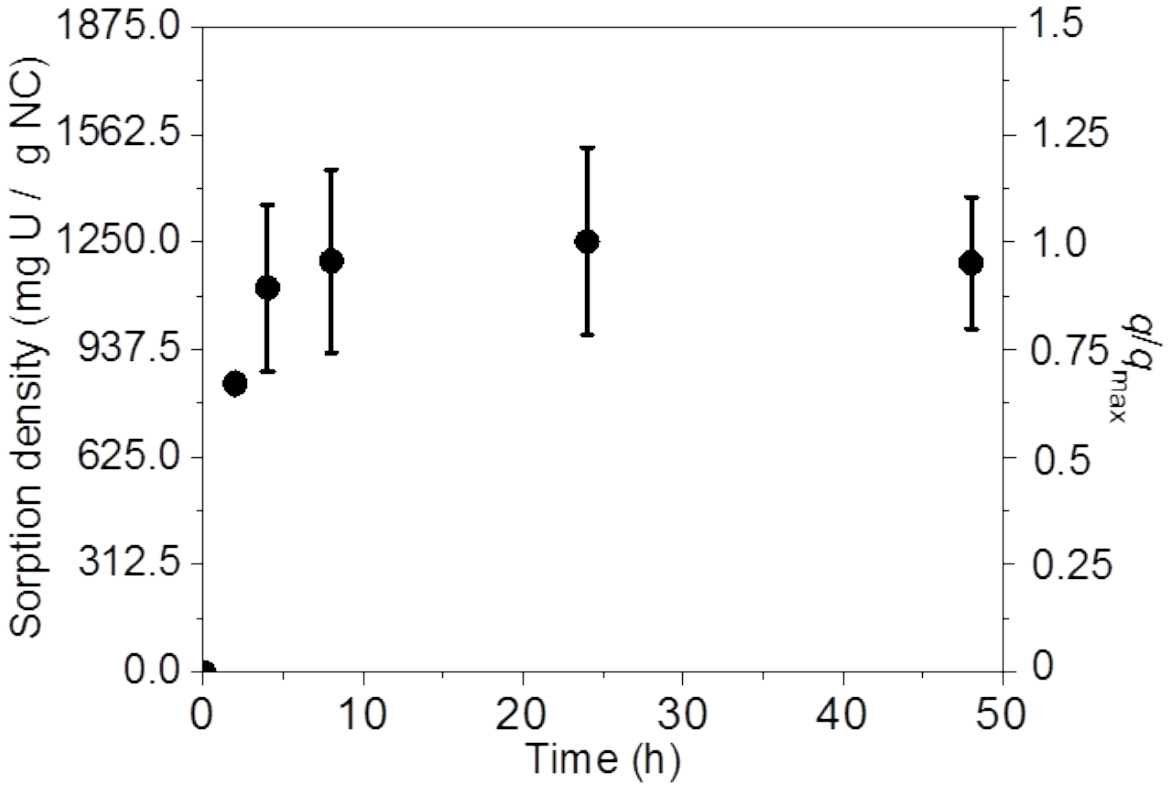

Fig S10. Equilibrium kinetics of a typical uranium sorption experiment. The number of $MnFe_2O_4$@OP nanocrystals used in the uranium sorption equilibrium kinetics was 5.1×10^{14} nanocrystals/L, which is 4 times lower concentration than the condition used in the uranium sorption experiment in the manuscript (2.3×10^{15} nanocrystals/L) and the initial concentration injected to the nanocrystal sample was 4 ppm of uranyl (VI) nitrate. The sorbed amount of uranium on the nanocrystal samples were monitored as a function of time while adjusting pH at 7.0 for 48 h and the experiments were repeated in triplicate.

Table S1. The maximum uranium sorption capacity (q_{max}, milligram of uranium per gram of nanocrystals), and the adsorption constant (k, liter per milligram) of pegylated and commercialized $MnFe_2O_4$ nanocrystal samples at pH 5.6, 7.0, and 8.5.

	$MnFe_2O_4$@PEG200			Commercial $MnFe_2O_4$		
pH	5.6	7.0	8.5	5.6	7.0	8.5
q_{max} (mg of U/g of NC)	217.4	140.8	91.7	7.5	6.6	4.9
K (L/mg)	0.8	1.3	1.6	1.6	7.2	0.5

Table S2. The maximum uranium sorption capacity (q_{max}, milligram of uranium per gram of nanocrystals), and the adsorption constant (k, liter per milligram) of bilayer structured (unsaturated saturate carbon chain linked) $MnFe_2O_4$ nanocrystal samples coated with octadecylphosphonic acid (ODP), stearic acid (SA), octadecylsulfate (ODS), and CTAB at pH 5.6, 7.0, and 8.5.

	$MnFe_2O_4$@ODP			$MnFe_2O_4$@SA			$MnFe_2O_4$@ODS			$MnFe_2O_4$@CTAB		
pH	5.6	7.0	8.5	5.6	7.0	8.5	5.6	7.0	8.5	5.6	7.0	8.5
q_{max} (mg of U/g of NC)	1111.1	1000	909.1	666.7	555.6	416.7	416.7	400.0	285.7	178.6	172.4	151.5
K (L/mg)	4.5	5	2.2	0.8	1.4	4.8	1.3	1.4	0.4	6.2	9.6	9.4

Table S3. The maximum uranium sorption capacity (q_{max}, milligram of uranium per gram of nanocrystals), and the adsorption constant (k, liter per milligram) of bilayer structured (unsaturated unsaturate carbon chain linked) $MnFe_2O_4$ nanocrystal samples coated with oleyl phosphate (OP) and oleic acid (OA) at pH 5.6, 7.0, and 8.5.

	$MnFe_2O_4$@OP			$MnFe_2O_4$@OA		
pH	5.6	7.0	8.5	5.6	7.0	8.5
q_{max} (mg of U/g of NC)	1666.7	1250	1000	909.1	666.7	434.8
K (L/mg)	0.9	1.4	0.7	1.1	1.1	0.2

Table S4. The maximum uranium sorption capacity (q_{max}, milligram of uranium per gram of nanocrystals), and the adsorption constant (k, liter per milligram) of oleic acid (OA) bilayer structured (unsaturated unsaturate carbon chain linked) $MnFe_2O_4$ nanocrystal samples at pH 7.0.

	MnO@OA	Mn_2FeO_4@OA	$MnFe_2O_4$@OA	Fe_3O_4@OA
q_{max} (mg of U/g of NC)	270.3	312.5	666.7	344.8
K (L/mg)	0.5	0.3	1.1	5.8

Table S5. XPS binding energies of individual peaks of the uranium 4f spectrum for the sample before and after uranium sorption. The concentration of each of oxidation state of U(IV) and U(VI) is V_1+V_3 and V_2+V_4, respectively

Sample	V_1	V_2	V_3	V_4	%U(IV)/U(VI)
$MnFe_2O_4$@OA-U	35.30 (380.97)	24.54 (381.89)	29.55 (391.77)	10.60 (392.71)	64.9/35.1
Fe_3O_4@OA-U	33.50 (380.55)	25.04 (381.60)	24.78 (391.23)	16.68 (392.13)	58.3/41.7
Mn_2FeO_4@OA-U	32.56 (380.81)	27.40 (381.79)	20.65 (391.70)	19.39 (392.60)	53.2/46.8
Mn_xO_y@OP-U	29.73 (380.86)	29.60 (381.84)	21.27 (391.63)	19.40 (392.67)	51.0/49.0
Uranium nitrate	0.00 (380.57)	58.60 (381.71)	0.00 (391.23)	41.40 (392.55)	0.00/100

Table S6. XPS binding energies of individual peaks of the iron 2P spectrum for the sample before and after uranium sorption. The concentration of each of oxidation state of Fe(II)/Fe(III) is $(V_\alpha)/(V_\beta)$.

Sample	V_α	V_β	%Fe(II)/Fe(III)
$MnFe_2O_4$@OA-U	27.69 (709.50)	72.31 (710.77)	27.7/72.3
$MnFe_2O_4$@OA	65.48 (709.87)	34.52 (711.94)	65.5/34.5
Fe_3O_4@OA-U	28.21 (709.57)	71.79 (710.89)	28.2/71.8
Fe_3O_4@OA	71.33 (709.93)	28.67 (711.98)	71.3/28.7
Mn_2FeO_4@OA-U	25.70 (709.08)	74.30 (710.51)	25.7/74.3
Mn_2FeO_4@OA	27.67 (709.79)	72.33 (711.05)	27.7/72.3

Table S7. XPS binding energies of individual peaks of the manganese 2P spectrum for the sample before and after uranium sorption. The concentration of each of oxidation state of Mn(II), Mn(III), and Mn(IV) is V_c+V_f, V_d+V_g, and V_e+V_h, respectively.

Sample	V_c	V_d	V_e	V_f	V_g	V_h	%Mn(II)/Mn(III)/Mn(IV)
$MnFe_2O_4$@OA-U	12.2 (639.7)	55.0 (641.2)	9.2 (643.8)	5.6 (651.4)	9.6 (652.6)	8.4 (653.6)	17.8/64.6/17.6
$MnFe_2O_4$@OA	26.5 (639.8)	30.0 (641.2)	14.4 (643.5)	8.2 (651.2)	15.5 (652.7)	5.5 (654.3)	34.7/45.5/19.9
Mn_2FeO_4@OA-U	14.4 (639.5)	45.6 (641.0)	11.0 (643.1)	7.8 (651.0)	17.6 (652.6)	3.6 (654.2)	22.2/63.2/14.6
Mn_2FeO_4@OA	16.8 (640.1)	37.0 (641.4)	16.8 (643.1)	9.5 (651.5)	12.7 (652.9)	7.2 (654.2)	26.3/49.7/24.0
Mn_xO_y@OA-U	7.5 (640.5)	57.2 (641.4)	13.4 (643.3)	7.4 (652.7)	8.2 (653.6)	6.2 (654.5)	15.1/65.4/19.6
Mn_xO_y@OA	15.1 (640.4)	45.6 (641.7)	12.0 (643.7)	6.2 (652.0)	15.2 (653.3)	6.1 (654.9)	21.3/60.8/18.0

Table S8. The maximum uranium sorption capacity (q_{max}, milligram of uranium per gram of nanocrystals), and the adsorption constant (k, liter per milligram) of oleylphosphate (OP) coated $MnFe_2O_4$ nanocrystal samples at pH 7.0 under varied sodium and calcium conditions.

$MnFe_2O_4$@OP, pH = 7.0								
Ionic condition (ppm)	Na 23	Na 229.9	Na 2299	Na 11494.9	Na 18391.8	Ca 6.5	Ca 27.2	Ca 51.3
q_{max} (mg of U/g of NC)	1250	1111.1	1111.1	1000	1000	1000	833.3	714.3
K (L/mg)	1	1.5	1.3	1.4	1.3	1.3	1.2	2.3

Table S9. The maximum uranium sorption capacity (q_{max}, milligram of uranium per gram of nanocrystals), and the adsorption constant (k, liter per milligram) of oleylphosphate (OP) coated $MnFe_2O_4$ nanocrystal samples at pH 7.0 in the presence of both sodium and calcium in water.

$MnFe_2O_4$@OP, pH = 7.0						
Ionic condition Na/Ca (ppm)	0/0	23.8/6.5	80.6/17.4	127.7/27.2	167/32.7	235.4/51.3
q_{max} (mg of U/g of NC)	1250	833.3	714.3	714.3	714.3	555.6
K (L/mg)	1.4	4	7	7	3.5	9